Signal-amplified Immunoassay Based on Biometallization of Palladium Nanoparticles and Nickel-Phosphorus Enhancement

Xinli Guo, Ping Zhang, Xinliang Liu, Na Zhang, Meihua Jiang, Qi Kang[*], Dazhong Shen[*]

College of Chemistry, Chemical Engineering and Materials Science, Collaborative Innovation Center of Functionalized Probes for Chemical Imaging in Universities of Shandong, Key Laboratory of Molecular and Nano Probes, Ministry of Education, Shandong Provincial Key Laboratory of Clean Production of Fine Chemicals, Shandong Normal University, Jinan 250014, P. R. China.
[*]E-mail:qikang@sdu.edu.cn; dzshen@sdnu.edu.cn

A sensitive electrochemical immunosensor was reported with signal amplification by biometallization of Ni-P. In this strategy, the primary antibody probes were immobilized on the aminated glass surface to bond the target antigen. Bounding with alkaline phosphatase (ALP) conjugated second antibody, the sandwich-type immunocomplex was formed. The signal tag of ALP in the immunocomplex can catalyze its substrate of *p*-aminophenyl phosphate to produce p-aminophenol, which can reduce Pd(II) in solution to Pd nanocrystals onto the surface. The Pd nanocrystals were served as the catalyst for electroless deposition of Ni-P layer in a successive signal amplification stage. Dissolved by HNO3, the amount of Ni deposited was determination by adsorptive stripping voltammetry method to quantify the target antigen. With human IgG as the model antigen, the applicability of the method was exploited. By using a bismuth nanoparticles modified glassy carbon electrode for Ni determination, the effect of the concentrations of *p*-aminophenol and Pd(II), biometallization time and temperature on the electroless deposition Ni-P were investigated and optimized. The stripping peak current of Ni was proportional to the concentration of human IgG in a dynamic range of 0.1–100 pg/mL with a detection limit of 0.03 pg/mL.

1. INTRODUCTION

A biosensor for cancer diagnosis usually consists of biomarker (target molecule), bioreceptor (recognition element) and compatible biotransducer [1].Various immunosensors are been developing to meet the increasing requests in sensitivity, selectivity, speed, accuracy and automatization [2,3]. To produce a detection signal, different labels including enzymes, chromophores, fluorophores and electrochemical probes have been explored in immunoassay [4]. Owing to its high sensitivity and

specificity in the biomarker detection, electrochemical immunosensors have received much attention [5-9]. Stripping voltammetry has been recognized as a powerful electrochemical technique for sensitive and rapid analyses of metal ions [10–12]. By combining with labeling by metal-related materials, the electrochemical immunosensors with high sensitivity were reported [13,14]. On the other hand, various signal amplification strategies have been proposed to enhance further the sensitivity of the electrochemical immunosensors [15-17]..

Biometallization is proved to be a promising strategy to improve the sensitivity of electrochemical [18] and colorimetric [19] biosensors. In this strategy, an enzyme-labeled second antibody or DNA probe is used to form the sandwich-type immunocomplex or DNA hybrid, which can catalyze a substrate to produce a reducing agent for metallic deposition. Alkaline phosphatase (ALP) is one of the most used enzymatic labels for the development of immunosensors and DNA hybridization assays. The hydrolysis products of ALP substrates such as *p*-aminophenyl phosphate (*p*-APP), 3-indoxyl phosphate and ascorbic acid 2-phosphate are known to be versatile reducing agents, and they can reduce silver cation to produce a silver deposition, which is quantified by the stripping or impedance measurements [20-26]. But the relative high background signals restrict the enhancement factor to be less than 80 in the successively silver deposition from the silver-enhancing solution [27].
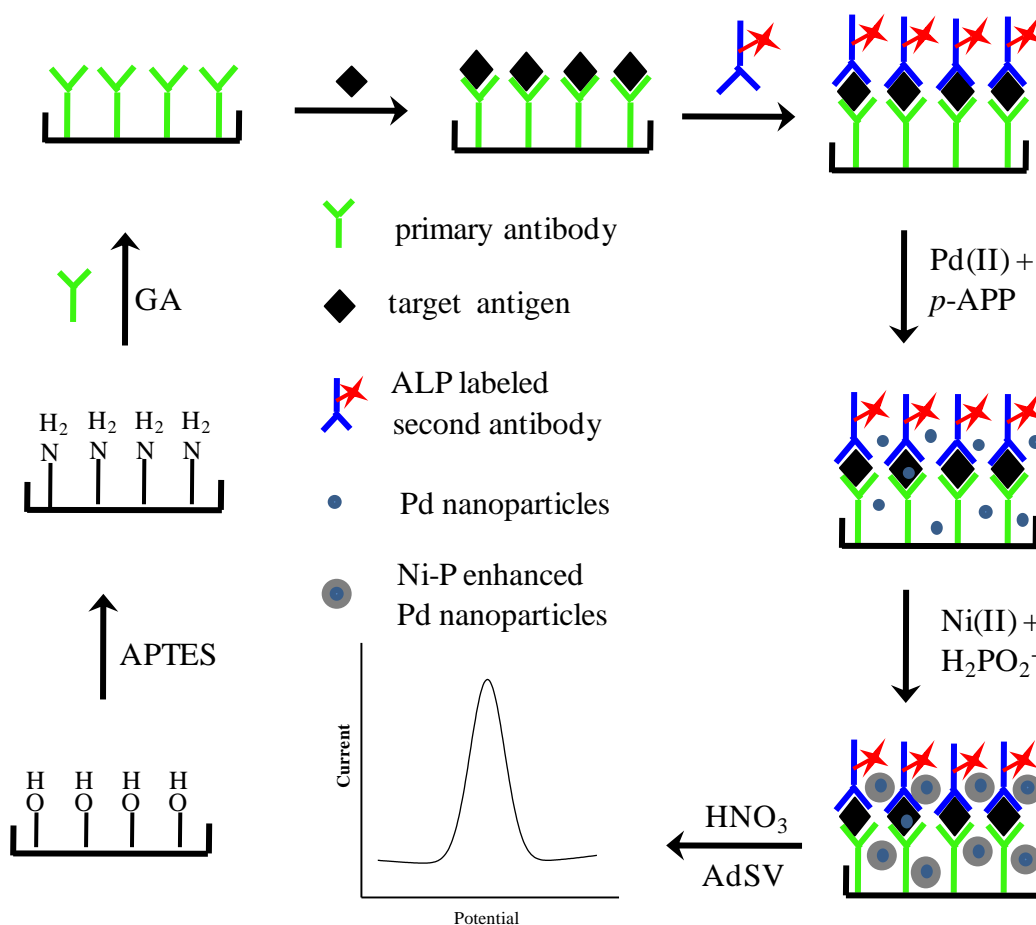

Figure 1. Scheme of electrochemical immunosensor with signal amplification by biometallization of Pd NPs and electroless deposition of Ni-P.

The aim of this research is to exploit the sensitivity enhancement for electrochemical immunosensors based on the biometallization strategy. With human immunoglobulin G (HIgG) chosen as the model analyte, the detection protocol is outlined in Figure 1. The primary antibody probes were immobilized on an aminated glass surface. After bounding with the corresponding antigen and ALP conjugated second antibody, Pd(II) in solution was reduced to palladium nanocrystals (Pd NCs) onto the glass surface by *p*-aminophenol (*p*-AP), which was generated from the substrate of *p*-APP by the catalysis of ALP in the sandwich-type immunocomplex. To enhance the sensitivity further, the deposited Pd NCs was served again as a signal tag and a high efficiency catalyst in the electroless plating nickel-phosphorus (Ni-P) layer for successive signal-amplification. The Ni-P enhancement layer is chosen because the activation energy in the electroless deposition of Ni-P from the mixture of Ni(II) ions and hypophosphite is relatively high [28], which is helpful to improve the signal-to-noise ratio for immunosensors based on biometallization strategy. Without a catalyst such as Pd NCs, the deposition rate of Ni-P is very small, especially at low temperature solution. Hence, the Ni-P enhancement is superior to silver enhancement approach in the much lower background level. The Ni-P particles were dissolved by HNO_3 and quantified by an absorption stripping voltammetry (AdSV) method. By using a bismuth nanoparticles (Bi NCs) modified glassy carbon electrode as the working electrode, the stripping peak current was proportional to the concentration of HIgG in a dynamic range of 0.1–100 pg/ml with a detection limit of 0.03 pg/mL.

2. EXPERIMENTAL

2.1 Chemicals and instruments

All chemicals were of analytical-reagent grade and used as received. All solutions were prepared with deionized and distilled water (from quartz). Glutaraldehyde (GA), *p*-aminophenyl phosphate monohydrate (p-APP), 3-Aminopropyltriethoxysilane (APTES), bovine serum albumin (BSA), dimethylglyoxime (DMG),N-hydroxysuccinimide (NHS), N-(3-dimethylaminopropyl)-N′-ethylcarbodiimide hydrochloride (EDC) and Nafion (5 wt% solution in a mixture of ethanol and water) were purchased from Sigma-Aldrich (Shanghai, China). Goat anti-human IgG antibody, human IgG, and ALP conjugated goat anti-human IgG antibody were purchased from Beijing Dingguo Biotechnology Development Center (Beijing, China). Other inorganic chemicals were obtained from Shanghai Aladdin Reagents Company (China).

The morphological evaluation was recorded by a transmission electron microscopy (TEM, JEM-1230, operating at 100kV). The electrochemical experiments were out in a conventional three-electrode cell controlled by a CHI660C workstation (Chenhua Instruments, China). A Bi NCs/Nafion modified glassy carbon electrode (Bi NCs/Nafion/GCE) was used as the working electrode, with an Ag/AgCl (saturated KCl) electrode and a platinum foil served as the reference electrode and auxiliary electrode, respectively.

2.2. Immunoassay procedure

The detection protocol of the successively signal-amplified electrochemical immunoassay is outlined in Figure 1. The purpose-designed glass chip with twelve cells (diameter 12 mm, volume 0.3 mL) was pretreated by the mixture of H_2SO_4+ H_2O_2 (3:1) for hydroxyl groups activation. Then, 150 μL 5 % APTES in ethanol was added into each cell to aminate the glass surface. After dried at 150 °C for 2 h, the aminated surface was activated with 2.5% GA (in pH 7.4 phosphate buffer) for 2 h and washing with water. Then 50 μL of 0.5 mg/mL anti-HIgG were applied to immobilize capture antibody on the aminated surface through cross-linking by GA. The immobilization was performed at room temperature for 60 min and then 4 °C overnight in a 100% moisture-saturated environment. Then the antibodies in physical adsorption were removed by washing with phosphate buffer saline (PBS, pH7.4) carefully. 150 μL of 1% BSA solution (dissolved in PBS) was added to block the active sites of the surface at 37 °C for 1 h. After that, 50 μL of different concentration of HIgG standard solutions were added into the cells and incubated at 37 °C for another 1h. After removal of the unbound by was with PBS three times, the resultant immunosensor was further incubated with ALP-labeled second antibody for 1 h to construct a sandwich-type immunocomplex. Subsequently, excess antibodies were washed with pH 7.2 Tris-HNO₃. 150 μL of enzyme reaction solution was added into the detection cell, on which Pd NCs were accumulated at 37°C for 40 min. The enzyme reaction solution was a glycine– NaOH buffer (pH 8.8) containing 1.5 mM *p*-APP and 0.8 mM $PdCl_2$, 1 mM $MgCl_2$. After that, the detection cells was washed with PBS containing 1 mM EDTA solution to remove Pd(II) in physical adsorption.

After deposition of Pd NCs as the catalyst, the glass chips were immersed in a nickel-enhancing solution to deposit the Ni-P layer. The Ni-P enhancing solution was composed by 26 g/L $NiSO_4 \cdot 6H_2O$, 31g/L $NaH_2PO_2 \cdot H_2O$, 29 g/L $C_6H_5Na_3O_7 \cdot 2H_2O$ and 19 g/L CH_3COONa and the pH was adjusted to 6.5 with acetic acid solution. The electroless deposition of Ni-P was performed at 37 °C for 60 min. Finally, the amount of Ni deposited on the sensing surface was quantified by AdSV method.
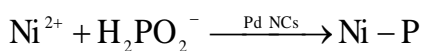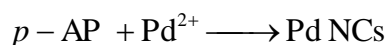
2.3. Electrochemical determination

The Bi NCs/Nafion/GCE was prepared according to a previous paper [29]. After the Ni-P particles on the surface of the immunocomplex was completely dissolved by 100 μL 5 M HNO₃, the solution was transferred into the into the voltammetric cell, next 2.0 mL of 1 M ammonia buffer (pH 8.2), 0.025 mL of 0.01 M DMG and 0.500 mL of 4 M NaNO₂ were added, and the total volume of the test solution was finally made up to 5 mL with ultrapure water. In the AdSV experiment, the complex of Ni-DMG was enriched on Bi NCs/Nafion/GCE at potential of − 0.7 V vs. Ag/AgCl for accumulation time of 240 s with stirring. The stripping current signal was recorded from −0.75 to -1.15 V at a scan rate of 100 mV s^{-1}. A baseline subtraction was carried out according to the reference [30]. With the currents in blank solution as the references, the changes in stripping peak current (ΔI) were calculated as the response to quantify Ni(II) as well as HIgG.

3. RESULTS AND DISCUSSION

3.1 Successive signal amlification in biometallization-based immunoassay

Figure 1 displays the working principle of the biometallization based immunoassay. First, the sandwich-type immunocomplex was formed on an aminated glass surface via the interaction between the target antigen and corresponding primary and secondary antibodies. Second, the signal tag of ALP in the immunocomplex converts *p*-APP to p-AP, which can reduce Pd^{2+} in solution to Pd NCs in the palladium enhancing solution. Under optimized conditions, the amount of Pd NCs deposited is related to the concentration of target antigen. Subsequently, the Pd NCs were served as signal tag again and the initial catalyzer for electroless deposition Ni-P. Finally, the amount of Ni deposited, which is related also to the concentration of target antigen, was detected by an AdSV method. The main reactions can be expressed as follows:

$$p - \text{APP} \xrightarrow{\text{ALP}} p - \text{AP}$$

$$p - \text{AP} + Pd^{2+} \longrightarrow \text{Pd NCs}$$

$$Ni^{2+} + H_2PO_2^{-} \xrightarrow{\text{Pd NCs}} Ni - P$$

By using a successive signal amplification strategy, the sensitivity for immunoassay is expected to improve significantly. Figure 2 shows the TEM images of Pd NCs and Pd-promoted Ni-P particles, it can be seen that Pd NCs is an effective catalyst for Ni-P deposition. But the key of such enhancing strategy is that the electroless deposition of Ni-P particles should be catalyzed only by Pd NCs, which was reduced only by *p*-AP produced in an enzyme-catalytic reaction.
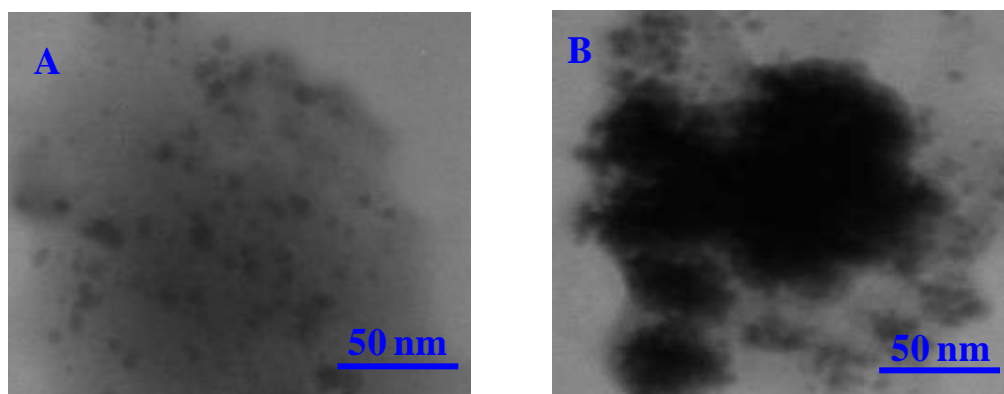

A

B

50 nm

50 nm

Figure 2. The TEM images of the Pd nanocrystals (A) and Pd-promoted Ni-P particles (B).

3.2 Electrochemical performance of Bi NPs/Nafion/GCE

In this work, the amount of Ni deposited was quantified by an AdSV method by using Bi NCs/Nafion/GCE due to its high sensitivity to Ni(II). It is well known that stripping voltammetry based on bismuth based electrodes offers high sensitivity comparable to mercury electrode and much

lower environmental toxicity [31-40]. As depicted in Figure 3, the complex of Ni-DMG exhibits well shaped voltammograms. Under our experimental conditions, the calibration plot was linear from 1 to 100 nM with a detections limit of 0.3 nM. The good sensitivity and repeatability makes the Bi NCs/Nafion/GCE a useful electrochemical sensor for nickel-based biometallization immunoanalysis.
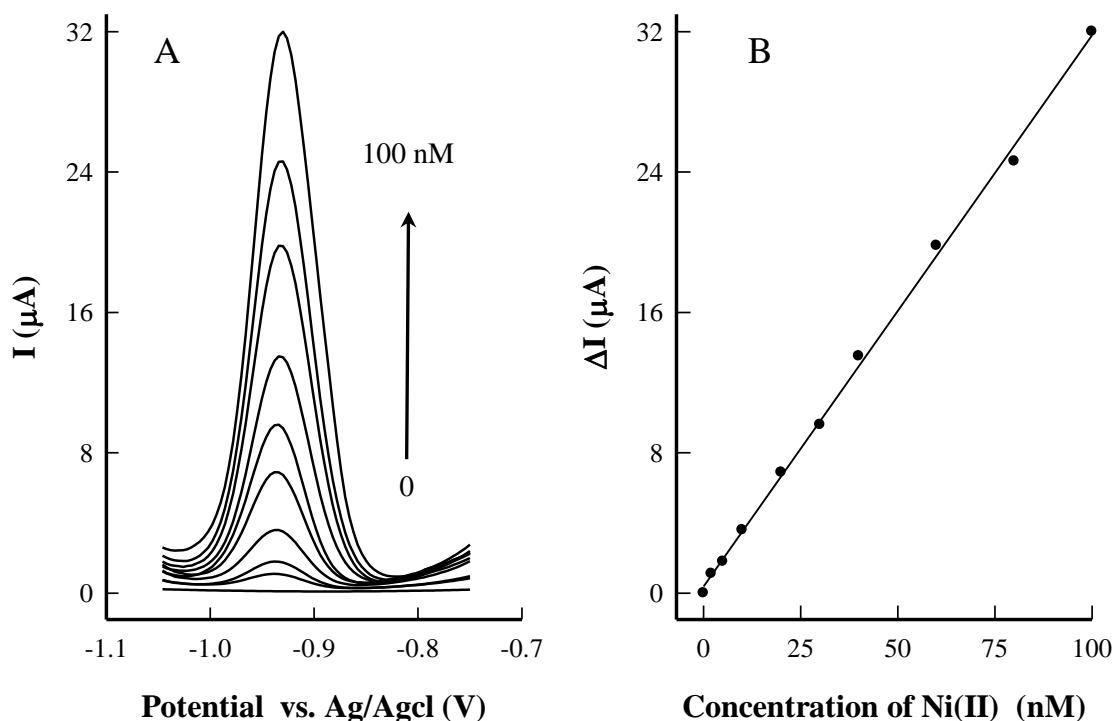

Figure 3. (A) AdSV voltammograms obtained at the Bi ABE for (A) and corresponding calibration plots (B).

3.3 Optimization for biometallization of Pd NCs

As a catalyst for the sequential Ni-P reducing, the amount, structure and dimensional distribution are expected to influence the performance of proposed the immunoanalysis method. To optimize the deposition of Pd NCs, the concentrations of *p*-APP and Pd(II) as well as the biocatalytical time in the biometallization stage were tested. As shown in Figure 4, the stripping peak currents are increased with increasing concentrations of *p*-APP or Pd(II), revealing that more Pd NCs are deposited at higher concentrations of *p*-AP or Pd(II). With the concentrations of *p*-APP up to 1.5 mM and Pd(II) up to 0.8 mM, the enhancement approaches to stabilize. Accordingly, 1.5 *p*-APP and 0.8 mM Pd(II) were adopted in the subsequent experiments.

As shown in Figure 5, the peak currents are increased with prolonged biocatalytic time, indicating the benefit for signal enhancement. With increasing biocatalytic time, more *p*-AP is expected to produce and more Pd NCs are deposited. But the activity of ALP may be decreased with increasing Pd NCs deposited. On the other hand, the size of the Pd NCs is expected to enlarge with
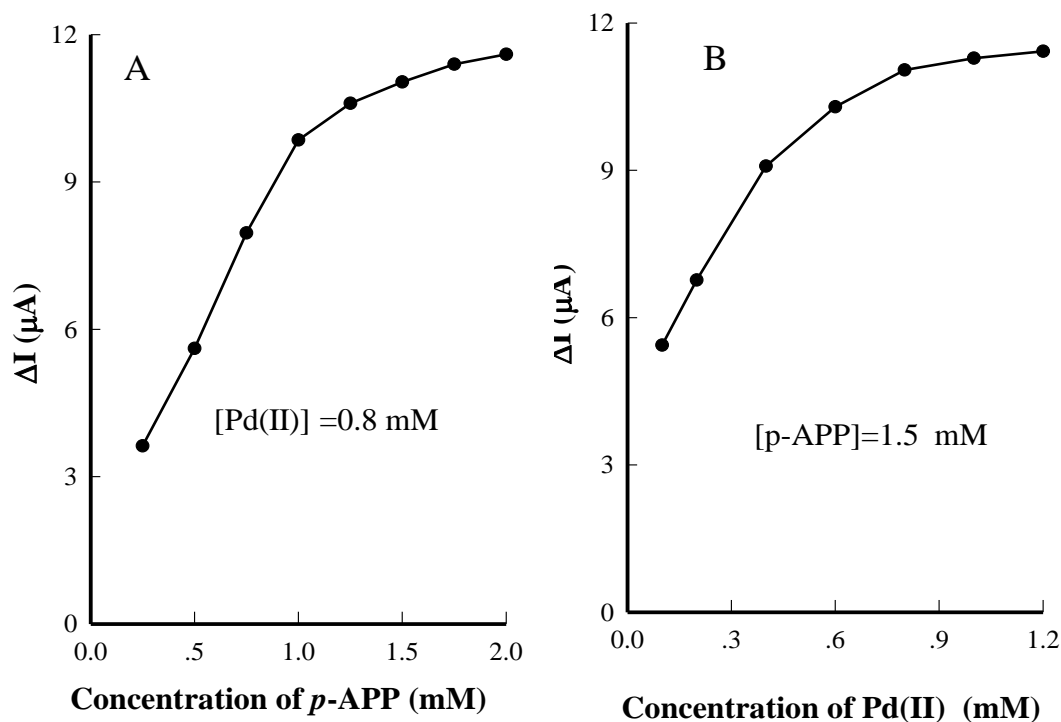
Figure 4. The effect of the concentration of *p*-APP (A) and Pd(II) (B) on the stripping peak current with Pd NCs and Ni-P signal amplification. Experimental conditions: [HIgG]=10 pg/mL, biocatalytic deposition time=40 min, Ni-P deposition time =60 min (37°C, pH=6.5).
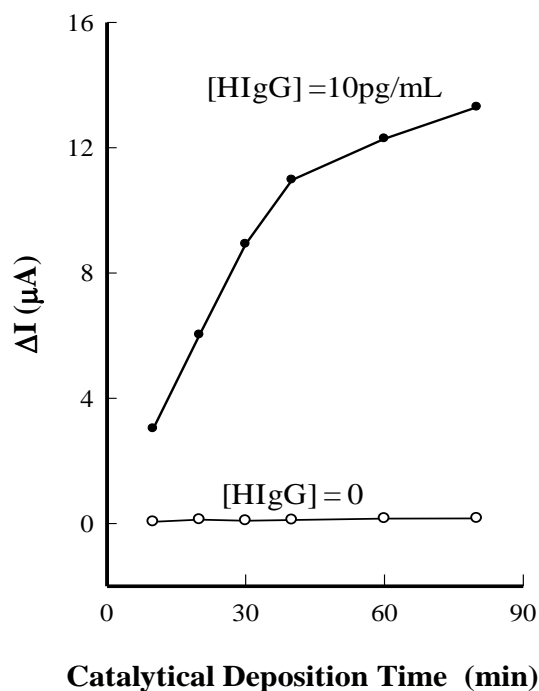

Figure 5. The effect of the biocatalytical time on stripping peak currents of the electrochemical immunosensor with Pd NPs and Ni-P signal amplification .Ni-P deposition time =60 min (37°C, pH=6.5).

increasing growth time, reducing the averaged catalytic activity in per mass of Pd NCs. As a result, the increase rate of the current is decayed gradually. Importantly, the increase in the background currents in the control experiment without the immunocomplex is slight, revealing that most of the Pd NCs are reduced by *p*-AP in the enzyme enhancing solution. This result is reasonable because Pd(II) solution itself has high chemical stability under the conditions used in this work. The photolysis of Pd(II) to Pd NCs is negligible, which is superior to the silver enhancing solution. On the other hand, the stability constant of the complex of Pd-EDTA is in about 10^{25} [41]. By washing with EDTA solution, Pd(II) in physical adsorption is removed to eliminate the Pd NCs reduced by HPO_2^- in the Ni-P deposition stage. Hence, the Pd NCs can be used as the signal tag in the successive amplification. Compromised between the sensitivity and analysis time, a biocatalytic time of 40 min was chosen in the following experiments.

3.4 Optimization for electroless deposition of Ni-P layer

With Pd NCs produced in biometalization stage as the catalytic activity center, an electroless deposition of Ni-P alloy was initiated. The overall reaction is given by:

$$Ni^{2+} + H_2PO_2^- + H_2O \rightarrow Ni\text{-}P + H_2 + 3H_2 PO_3^- + H^+$$

Note that the Ni-P particles or layer deposited have an autocatalytic effect, which can make the deposition reaction to proceed automatically. Hence, a high enhancement factor can be achieved and the sensitivity of the immunosensor is expected to improve significantly. To optimize the deposition of Ni-P, the influences of pH, temperature and deposition time were tested. As can be seen in Figure 6,
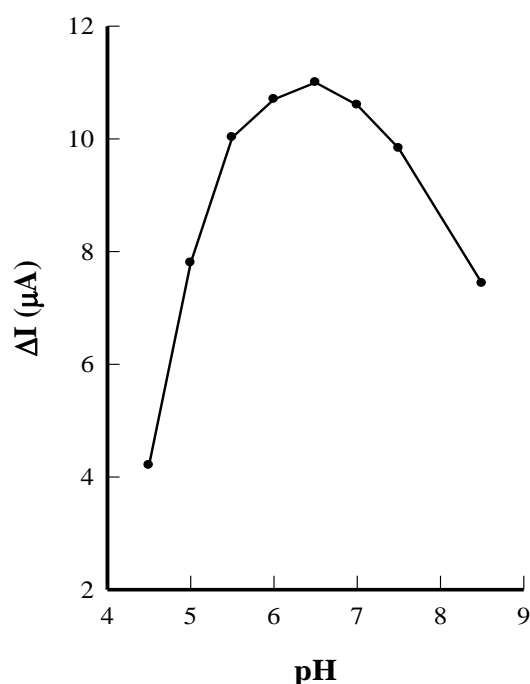

Figure 6. The effect of the pH in electroless deposition of Ni-P on the stripping peak current of with PdNPs and Ni-P signal amplification. Other experimental conditions as same as Figure 4.

the maximum peak current was obtained in the enhancing solution of pH 6.5 Accordingly, pH=6.5 was chosen for Ni-P deposition in the successive amplification stage.

Usually, electroless deposition Ni-P alloy is performed at 70−90 °C to increase the growth rate for the coatings in the mechanical, petrochemical, aerospace, automobile, microelectronics and semiconductor industries [42,43]. In this work, we employed a low temperature formula for electroless deposition Ni-P for two reasons. One is to reduce the decomposition of the nickel enhancing solution, suppressing the deposition of Ni without Pd NCs catalysis and the background level the immunosensors. Another is that the biosensing layer on the glass surface may be even peeled off in high temperature solution.

Figure 7 displays the influence of temperature on the response of the immunosensor. It is clear that the rate of Ni-P deposition is increased with increasing temperature. The activity energy (E_a) can be estimated according to the Arrhenius's equation.

$$\ln r = \ln A_0 - \frac{E_a}{RT}$$

where r is averaged deposition rate, A_0 is a constant called the frequency factor, R is the universal gas constant, T is the temperature in Kelvin. The value of $E_a = 68.3$ kJ/mol is estimated for the electroless deposition of Ni-P under the conditions used in this work. The relative high activation energy offers the advantage of low background level in the Ni-P enhancement approach. As shown in Figure 7B, the background levels in the controls increased only slightly during the Ni-P deposition process, especially in the early stage. But the background level is risen in the later stage (t >2 h),
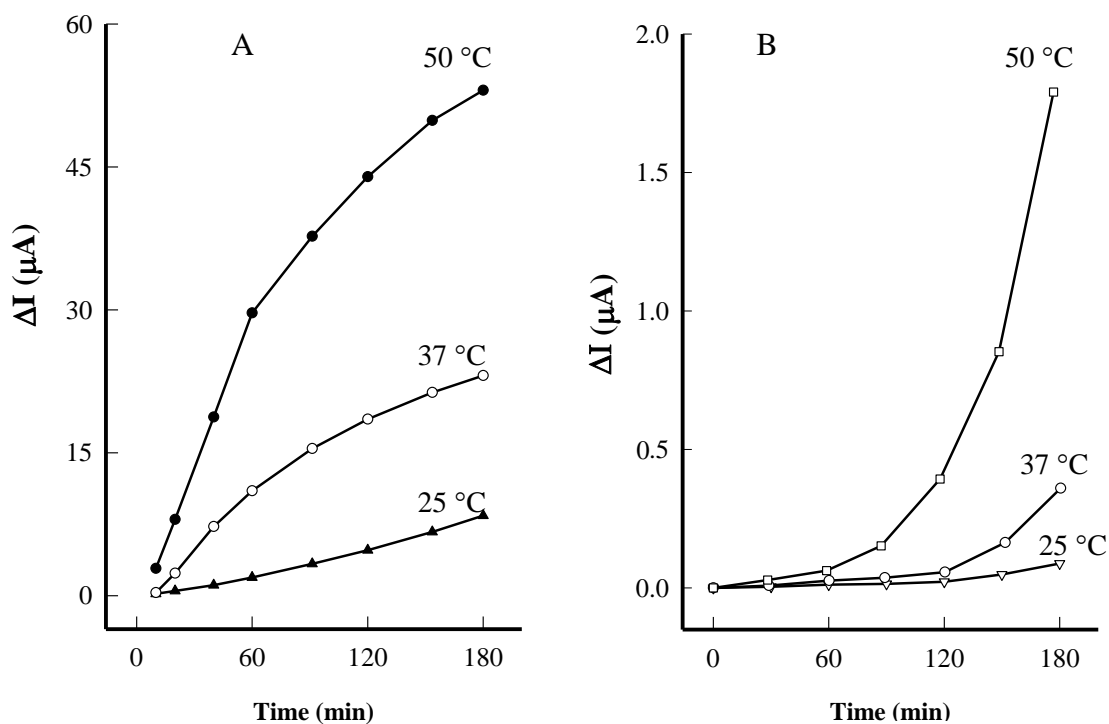

Figure 7. The changes in stripping peak currents in immunosensor with 10 pg/mL HIg G (A) and control without immunocomplex (B) at different temperature. Other experimental conditions as same as Figure 4.

especially at 50 °C. The reason may be that part of Ni-P particles were also produced after a long reaction time even in the absence of catalysis from Pd NCs. With Ni-P particles as the catalytic activity center, the Ni-P deposition process is accelerated gradually, resulting in the rise in background level. Based on the considerations of analysis time, sensitivity and background level, the deposition time of 60 min at 37 °C was chosen for the sequent immunoanalysis.

3.5. Analytical performance for determination of human IgG

In this work, we employed the signal amplification strategy based on the biometallization of Pd NCs and sequent electroless deposition of Ni-P. Under the optimized conditions, the calibration curve is depicted in Figure 8. It can be seen that the stripping currents are in linear correlation with the concentration of HIgG in double logarithmic coordinates. The linear range is 0.1~100 pg/mL with a LOD of 0.03 pg/mL. The comparison of the analytical performance of the developed method with other electrochemical immunosensors for HIgG detection is summarized in Table 1. It can be seen that the analytical performance of the developed method is comparable with other electrochemical immunosensors. Note that the sensitivity of the Ni-P signal enlargement strategy is obviously higher than that in a similar a successive signal amplification with silver enhancement [27]. Compared with silver enhancement system, the improvement in the sensitivity of the developed method may be ascribed to the higher chemical stability of Pd(II) and catalytic activity of Pd NCs, higher stability constant of Ni-EDTA, and high activation energy of in Ni-P deposition. Hence, a higher enhancement factor was obtained by using deposition time for Ni-P without an obvious rise in the background signals.
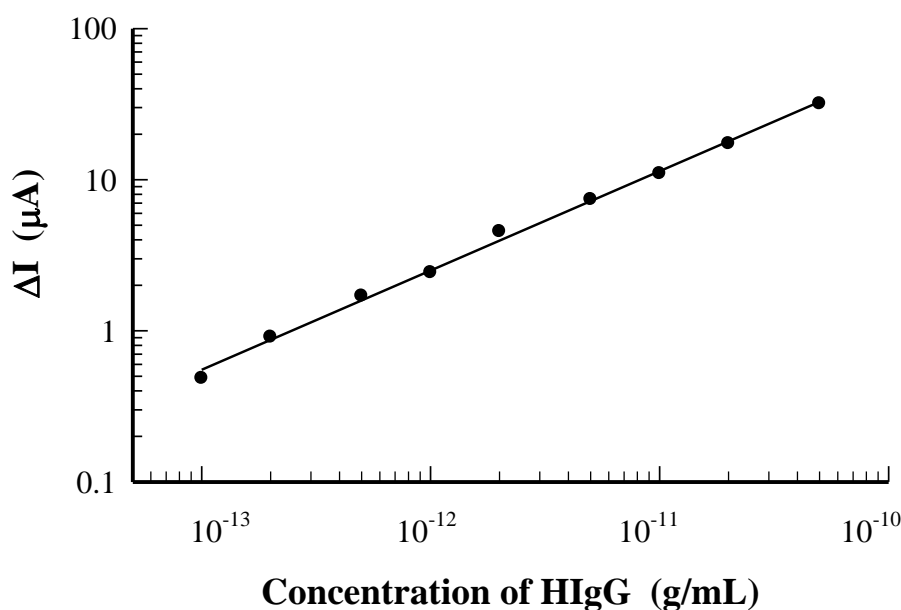

Figure 8. The calibration curve of the electrochemical immunosensor with successive signal amplification by Pd NPs and Ni-P deposition.

Table 1. Comparison of the analytical performance of the developed method with other HIgG electrochemical immunosensors.

Electrode	Signal amplification	Signal tag	Linear range ng/mL	LOD ng/mL	References
CdS/ITO	GOx-Au NPs	H_2O_2	$5-3\times10^2$	1.5	[44]
D-Fc/ITO	HRP–SiO$_2$	H_2O_2	$1.5-2\times10^3$	2.2	[45]
CNFs-Chit/GCE	Ag@Au-Fe$_3$O$_4$	H_2O_2	$10^{-4}-5\times10^3$	5×10^{-5}	[46]
avidin /ITO	enzyme label	$Ru(NH_3)_6^{3+}$	$0.1-10^2$	0.01	[47]
TTA/Au	enzyme label	HRP	0.01–25	0.003	[48]
DAC/GCE		$[Fe(CN)_6]^{4-/3-}$	0.5–45	0.3	[49]
Au NPs--rGO/SPCE	HRP-Au NPs	polyaniline	$0.02-5\times10^2$	0.01	[50]
Au NPs/SPCE	PB-MCN	PB	$0.01-1\times10^2$	0.008	[51]
Grapheme oxide/GCE	Cu@TiO$_2$	Cu^{2+}	$10^{-4}-10^2$	5×10^{-5}	[52]
SAM/Au	DNA–AuNPs	Ag	10^2-10^5	20	[53]
Au NPs-PDA-rGO/GCE	Ag NPs/C NC	Ag	$0.1-10^2$	0.0075	[54]
Magnetic GCE		Ag	$10^{-4}-5\times10^3$	5×10^{-5}	[55]
SPE	successively amplification	Ag^+	0.1–10	0.03	[27]
Bi NCs/Nafion/GCE	successively amplification	Ni^{2+}	$10^{-4}-0.1$	3×10^{-5}	This work

CNFs-Chit: carbon nanofibers-chitosan composite, C NC : carbon nanocomposite, DAC: dialdehyde cellulose, D-Fc: HRP–SiO2: horseradish peroxidase (HRP)-doped nanosilica particles, PB-MCN: Prussian blue (PB) functionalized mesoporous carbon nanosphere (MCN), PDA: polydopamine rGO: reduced graphene oxide TTA: thiol aromatic aldehyde.

In order to investigate the feasibility of the developed immunoassay for clinical analyses, it was applied to determine the level of HIgG in 18 human serum samples. The results were compared with those obtained by the standard enzyme-linked immunosorbent assay (ELISA) method. The correlation of the data in the two methods is expressed as: $C_1 = 1.037 + 1.052C_2$ ($R^2 = 0.958$), where C_1 and C_2 are the concentration measured by the ELISA and the developed methods, respectively. This result indicates that there is no significant difference between the results given by two methods. Hence, the developed immunoassay is feasible for detection of HIgG.

4. CONCLUSION

In summary, we developed a successively amplified electrochemical immunosensor utilizing the biometallization of Pd NCs and subsequent Ni-P alloy enhancement. A high sensitivity was obtained in the basis of the highly catalytic action of ALP and Pd NCs and automatic catalysis of Ni-P.

And a low background level is achieved due to the high chemical stability of Pd (II), high efficiency of Pd NCs and high activation energy of electroless deposition of Ni-P. The successive amplification strategy can improve the sensitivity of electrochemical immunosensor. The proposed signal amplification holds great promise for the extended applications in the field of bioaffinity assays based on biometallization strategy.

References

1. S. Mittal, H. Kaur, N. Gautam and A. K. Mantha, *Biosens. Bioelectron.*, 88 (2017) 217.
2. E.B.Bahadır and M. K. Sezgintürk, *Anal. Biochem.*,478 (2015) 107.
3. P. Mehrotra, *J. Oral Biol. Craniofacial Res.*, 6(2016) 153.
4. T. Wei,Z. Dai,Y. Lin and D. Du, *Electroanalysis,*28(2016) 4.
5. F. Ricci, G. Adornetto and G. Palleschi, *Electrochim. Acta*, 84 (2012) 74.
6. K. K.Mistry, K.Layek, A.Mahapatra,C.Roychaudhuri and H.Saha, *Analyst*, 139(2014) 22893
7. M. A. Arugula, Y. Zhang and A. L. Simonian, *Anal. Chem.* 86 (2014) 119.
8. H. Radecka and J. Radecki, *J. Mex. Chem. Soc.*, 59(2015)269.
9. B.Rezaei, M.Ghani, A.Mousavi S. and M.Rabiee, *Biosens. Bioelectron.*, 78(2016) 513.
10. C. A. Rusinek, A.Bange, M. Warren, W. Kang, K.Nahan, I.Papautsky and W. R. Heineman, *Anal. Chem.,* 88 (2016) 4221.
11. R. A. Segura, J. A. Pizarro, M.P. Oyarzun, A. D. Castillo, K.J. Díaz and A. B. Placencio, *Int. J. Electrochem. Sci.*, 11(2016) 1707.
12. M. I.Saidin, I. M. Isa, M.Ahmad , N.Hashim and S. A.Ghani, *Sens. Actuators* B, 240 (2017) 848.
13. M.Abdorahim, M.Rabiee,S. N.Alhosseini, M.Tahriri, S.Yazdanpanah,S. H.Alavi and L.Tayebi, *Trends Anal. Chem.,*82(2016) 337.
14. S.Shrivastava, N.Jadon and R. Jain, *Trends Anal. Chem.*, 82(2016)55.
15. H.X. Fan, Z.K. Guo, L. Gao, Y. Zhang, D.W. Fan, G.L. Ji, B. Du and Q. Wei, *Biosens. Bioelectron.,* 64 (2015) 51.
16. X.Y.Zhao, W. Liu, B.B. Zhou, S.S. Liu and G.C. Han, *Int. J. Electrochem. Sci.*, 10 (2015) 8910
17. S. A. Lim, M. U. Ahmedm, *RSC Adv.*, 6(2016) 24995.
18. S. Hwang, E. Kim and J.Kwak, *Anal. Chem.*,77 (2005) 579.
19. C.H. Zhou, J.Y. Zhao, D.W. Pang and Z.L.Zhang, *Anal.Chem.* , 86(2014) 2752.
20. Y. Luo, X.Mao, Z.F.Peng, J.H.i Jiang, G. L. Shen and R.Q. Yu, *Talanta*,74(2008) 1642.
21. P. Zhang, X. Chu, X.M.Xu, G.L.Shen and R.Q.Yu, *Biosens. Bioelectron.*, 23(2008) 1435.
22. B. A. Zaccheo and R. M. Crooks, *Anal. Chem.* ,81(2009) 5757.
23. T.H. Degefa, S. Hwang, D. Kwon, J.H. Park and J. Kwak, *Electrochim. Acta*, 54(2009) 6788
24. G.S. Lai, F.Yan, J.Wu, C.Leng and H.X.Ju, *Anal. Chem.*,83 (2011) 2726.
25. Y.M.Si, Z.Z. Sun, N. Zhang, W. Qi, S. Y. Li, L.J.Chen and H. Wang, *Anal. Chem.*, 86(2014) 10406.
26. A.M.J. Haque, J.Kim, G. Dutta, S.Kim and H.Yang, *Chem. Commun.*, 51 (2015) 14493.
27. Z.P. Chen, Z.F.Peng, Y.Luo, B.Qu,J.H. Jiang, X.B. Zhang, G.L.Shen and R.Q.Yu, *Biosen. Bioelectron.*, 23 (2007) 485.
28. W.L. Liu, S.H. Hsieh, T.K. Tsai, W.J. Chen and S. S. Wu, *Thin Solid Films*,510 (2006) 102.

29. S.J. Wu, W.J. Lu, K.Qi, D.Z.Shen and D.W. Pan, *Micro Nano Lett*., 7(2012) 1260.
30. B. Baś,K. Węgiel and K. Jedlińska, *Electrochim. Acta*,178(2015) 665.
31. J. Wang, J.M. Lu, S.B. Hocevar and P. A. M. Farias, *Anal. Chem*., 72 (2000) 3218.
32. J. Wang, *Electroanalysis* ,17(2005)15.
33. L.A. Piankova, N.A. Malakhova, N.Yu. Stozhko, Kh.Z. Brainina, A.M. Murzakaev and O.R. Timoshenkova, *Electrochem. Commun*.,13 (2011) 981.
34. H.Sopha, J. Roche, I. Švancara and A. Kuhn, *Anal. Chem*., 86 (2014) 10515.
35. B. Bas, K.Wegiel and K. Jedlinska, *Anal. Chim. Acta*,881(2015)44.
36. S. D. Borgo,H.Sopha, S. Smarzewska, S. B. Hocevar, I. Svancara and R. Metelka, *Electroanalysis*, 27(2015) 209.
37. G. Zhao, H. Wang and G. Liu, *Int. J. Electrochem. Sci*., 11 (2016) 1840 .
38. T. Romih, S. B. Hocevar , A. Jemec and D. Drobne, *Electrochim. Acta*, 188 (2016) 393.
39. G.J. Fan, D.S. Zhai and D.S. Zou, *Int. J. Electrochem. Sci.,* 11 2016) 4362.
40. R. A. Segura, J. A. Pizarro, M. P. Oyarzun, A. D. Castillo, K J. Díaz and A. B. Placencio, *Int. J. Electrochem. Sci*., 11 (2016) 1707.
41. J. Kragten,L.G. Decnop-Weever,J. Kragten and L.G. Decnop-Weever, *Talanta*, 30(1983) 449.
42. P. Sahoo,S. K. Das, *Mater. Design*., 32(2011) 1760.
43. J. Sudagar, J. Lian and W. Sha, *J. Alloy. Compd*.,571(2013) 183.
44. H.C. Pan, S. Huang, X.P. Li, P. Li and W.Y. Zhu, *Int. J. Electrochem. Sci*., 11 (2016) 3364.
45. Z.Y. Zhong, M.X. Li, D.B. Xiang, N. Dai, Y. Qing, D. Wang and D.P. Tang, *Biosen. Bioelectron*., 24 (2009) 2246.
46. H.F. Zhang, L.N. Ma, P.L. Li and J.B. Zheng, *Biosen. Bioelectron*., 85(2016) 343.
47. G. Dutta, S. Park, A. Singh, J. Seo, S. Kimand H.Yang, *Anal. Chem.* , 87(2015) 3574.
48. Y.M. Shen, Y.Y. Zhang, M.L. Liu, X.Y. Liu, H. Guo, X.Y. Zhang, C.X. Zhang, H.T. Li and S.Z. Yao, *Talanta*, 141(2015) 288.
49. X.Y. Zhang, G.Y. Shen, S.Y. Sun, Y.M. Shen, C.X. Zhang and A.G. Xiao, *Sens. Actuators B*, 200(2014) 304.
50. G.S. Lai,H.L. Zhang,T. Tamanna and A.M. Yu, *Anal. Chem.*, 86(2014) 1789.
51. G.S. Lai, H.L. Zhang, A.M. Yu and H.X. Ju, *Biosen. Bioelectron*., 74 (2015) 660.
52. S. Zhang, H.M. Ma, L.G. Yan, W.Cao, T.Yan, Q. Wei and B. Du , *Biosen. Bioelectron*., 59 (2014) 335.
53. X.Y. Li, Z. Y., H. Tang, X. Chu and R.Q. Yu, *Anal. Methods*, 6(2014) 2221.
54. S. Zhang, N. Huang, Q.J. Lu, M.L. Liu, H.T. Li, Y.Y. Zhang and S.Z. Yao, *Biosen. Bioelectron*., 77(2016) 1078.
55. P.L. Li and H.F. Zhang, *J.Chin.Chem.Soc*., 63(2016) 784.